

(Carrier Drift Modulation and the) Hyperbolic Time Crystals

Evgenii E. Narimanov¹ and Boris Shapiro²

¹*School of Electrical and Computer Engineering and Birck Nanotechnology Center,*

Purdue University, West Lafayette, Indiana 47907, USA and

²*Department of Physics, Technion - Israel Institute of Technology, Haifa 32000, Israel*

(Dated: January 5, 2026)

We introduce the Carrier Drift Modulation – a new mechanism for creating temporal boundaries and enabling photonic time crystals. This approach opens a direct route to hyperbolic temporal metamaterials and, in particular, hyperbolic time crystals. We demonstrate that the very process responsible for time crystal formation can simultaneously compensate intrinsic material losses in the supporting medium — overcoming one of the central challenges in nanophotonics. The realization of truly lossless hyperbolic media, long considered as one of the key challenges of nanophotonics, unlocks new possibilities for subwavelength light focusing, strong-field physics, and novel regimes of light–matter interaction. Crucially, the proposed approach can be implemented using existing materials and readily available light sources, making it both practical and transformative.

I. INTRODUCTION

Ultra-fast temporal modulation of an optical material [1] – where its electromagnetic properties are rapidly varied over time – creates dynamic boundaries that light can interact with, much like spatial interfaces in conventional optics.[2, 3] When these temporal changes occur faster than the oscillation period of the incident light, they give rise to distinctive phenomena known as time reflections and time refractions, in which photons experience abrupt changes in frequency and propagation direction, while their momentum remains conserved.[2–4] When such modulation is applied periodically, the system evolves into a photonic time crystal [5–12] – a medium with a repeating structure in time that enables novel forms of light control, from amplification to frequency conversion and precise manipulation of photonic states [8–10].

However, achieving optical modulation that is both strong and fast is a significant challenge, as balancing these extremes often strains material limits and device performance.[13] Yet, even relatively weak modulation can radically alter optical response when it induces a transition [14] – such as from the dielectric to the hyperbolic regime [15]. Crucially, such topological transitions occur only in anisotropic media [15], as isotropic materials cannot support hyperbolic dispersion [16].

Here we introduce a new approach to ultra-fast optical modulation capable of inducing a topological transition from elliptical to hyperbolic regimes in a fundamentally isotropic material. The proposed approach of Carrier Drift Modulation, shifts the velocity distribution of free charge carriers in the direction of the average electric field of an ultra-fast optical pump pulse. This free carrier drift creates a transient, pump-induced anisotropy, enabling an optically driven electromagnetic topological transition from an elliptic to a hyperbolic response.

Our approach not only offers a solution to the challenge of achieving strong modulation at ultra-fast timescales, but also opens the path to realizing a Hyperbolic Time Crystal – a photonic time crystal that inherits the ex-

otic properties of hyperbolic media. By inducing transient anisotropy in an otherwise isotropic material, Carrier Drift Modulation enables periodic temporal transitions into the hyperbolic regime, combining the dynamic control of time crystals with the high-wavenumber mode support and extreme light-matter interaction characteristics of hyperbolic materials.

With the proper choice of the temporal modulation period, the Hyperbolic Time Crystal can also support parametric amplification, when the energy from the modulation is transferred to the optical field. This gain mechanism offers a pathway to compensate for intrinsic material losses, long considered the fundamental limitation of hyperbolic media, with the potential to reach the Holy Grail of nanophotonics – the lossless hyperbolic medium.

II. CARRIER DRIFT MODULATION

An intense optical pulse propagating in a conducting sample, rapidly accelerates the free charge carriers – leading to a noticeable increase of their kinetic energy above the Fermi level. With the ever present band non-parabolicity inherent to all conducting materials, this immediately leads to a change of the free carrier response to a time-dependent probe field – offering a practical approach to ultra-fast modulation of electromagnetic response. In a typical setting of this framework, the high optical pump intensity that is necessary for strong modulation, is achieved by the optical time-compression of laser pulses – naturally leading to the eventual pulse duration τ_M that is relatively short on the “electronic” time scale τ_0 defined by the rate of the free carrier scattering, but well above the time of a single optical pump cycle $2\pi/\omega_M$:

$$\frac{2\pi}{\omega_M} \ll \tau_M \ll \tau_0. \quad (1)$$

In general, an optical pump pulse leads to both the “drift” of the free carriers in the direction of the applied electric field, $\langle \mathbf{p} \rangle \equiv \mathbf{p}_M \propto \mathbf{E}_M$, and to the increase

of their average energy $\Delta\langle\varepsilon_{\mathbf{p}}\rangle \propto \langle\mathbf{E}_M^2\rangle$. When $\tau_M \gg 2\pi/\omega_M$, multiple oscillation of the pump field rapidly average out the imposed carrier drift, $\mathbf{p}(t > \tau_M) \rightarrow 0$.

However, the situation is very different when using ultra-short pulses that last for only a few cycles – all the way to the unipolar (sub-cycle) fields [17] :

$$\tau_M \lesssim \frac{2\pi}{\omega_M} \ll \tau_0. \quad (2)$$

In this case, the drift momentum of the free carrier distribution imposed by the entire pump pulse, $\langle\mathbf{p}\rangle \neq 0$, immediately leading to an *anisotropic* electromagnetic response of the modulated medium.

The free carrier electromagnetic response strongly depends on the signal frequency ω ,

$$\text{Re}[\epsilon(\omega)] \propto 1 - \omega_p^2/\omega^2 \quad (3)$$

and changes sign at the plasma frequency ω_p that is defined by the free carrier dynamics. Therefore, the anisotropy of the dielectric permittivity tensor imposed by the drift modulation, implies the necessary existence of the frequency band where the modulation turn the originally isotropic response (dielectric when $\epsilon_\omega > 0$ and metallic when $\epsilon_\omega < 0$) into hyperbolic (for opposite signs of the permittivity components in the directions that are parallel and perpendicular to the modulating electric field). For such signal wavelength, the drift modulation introduced in the present work, will not simply quantitatively change the system parameters but will instead induce a *topological transition* [15] from elliptic to hyperbolic dispersion, that is known [15] to *qualitatively* change the electromagnetic response of the material.

The mechanism of the pump-induced anisotropy of the electromagnetic response of free carriers originates from the combined effect of the drift of the electron distribution in the direction defined by the average electric field of the pump pulse, and the energy band non-parabolicity. With the energy-dependent effective mass of the charge carriers, energy transferred from the pump to the free electrons, modifies their electromagnetic response [13]. A strongly anisotropic velocity distribution of the free electrons that was induced by the pump, will therefore result in an anisotropic non-parabolicity correction to the electromagnetic response – leading to the aforementioned transition in the appropriate frequency window. Furthermore, since the transition occurs at a time scale much faster than the electronic relaxation time τ_0 , irreversible processes cannot suppress it.

A timed sequence of short intense pulses incident on a conducting material (such as e.g., a doped semiconductor or a transparent conducting oxide (TCO) film), with the electric field $\mathbf{E}_M(\mathbf{r}, t)$ acting on the free electrons in the sample, creates a “hot electron” distribution $f_M(\mathbf{p}, t)$, which satisfies the kinetic equation [18]

$$\frac{\partial f_M}{\partial t} + \mathbf{v}_{\mathbf{p}} \cdot \nabla f_M + e\mathbf{E}_M(\mathbf{r}, t) \cdot \frac{\partial f_M}{\partial \mathbf{p}} = -\frac{f_M - f_0}{\tau_0}, \quad (4)$$

with the initial condition of the system being in the equilibrium at $t \rightarrow -\infty$:

$$f_M(\mathbf{p}, \mathbf{r}; t \rightarrow -\infty) = f_0(\mathbf{p}), \quad (5)$$

where $\mathbf{v}_{\mathbf{p}} \equiv \partial\varepsilon_{\mathbf{p}}/\partial\mathbf{p}$ is the charge carrier group velocity, and $f_0(\mathbf{p})$ is the equilibrium (Fermi-Dirac) distribution that is normalized to the free electron concentration n_0

$$\frac{2}{(2\pi\hbar)^3} \int d\mathbf{p} f_0(\mathbf{p}) = n_0. \quad (6)$$

The gradient term $\mathbf{v}_{\mathbf{p}} \cdot \nabla f_M$ in the kinetic equation (4) describes the spatial nonlocality of the electromagnetic response of the charge carriers, as the coordinate displacement of a free electron over the period of a single optical cycle, scales as v_F/ω_M , where v_F is the free electrons Fermi velocity. When $v_F \ll c$, this length scale is much smaller than the wavelength $\lambda_M \sim c/\omega_M$, and the spatial gradient term in the kinetic equation (4) can be neglected.

For the solution of Eqn. (4) with the initial condition (5) we therefore obtain

$$f_M = \int_{-\infty}^t \frac{dt'}{\tau_0} f_0(\mathbf{p} - \mathbf{p}_M(\mathbf{r}, t) + \mathbf{p}_M(\mathbf{r}, t')) e^{-\frac{t-t'}{\tau_0}}, \quad (7)$$

where $\mathbf{p}_M(\mathbf{r}, t)$ is the impulse that was transferred to the free electrons from the modulation field by the time t :

$$\mathbf{p}_M(\mathbf{r}, t) = e \int_{-\infty}^t \mathbf{E}_M(\mathbf{r}, t') dt'. \quad (8)$$

At the times shorter than the electronic relaxation, the solution (7) corresponds to the reversible dynamics of a collision-less plasma [19] under the action of the pump

$$f_M(\mathbf{p}, \mathbf{r}; t) = f_0(\mathbf{p} - \mathbf{p}_M(\mathbf{r}, t)), \quad (9)$$

with \mathbf{p}_M corresponding to the average (drift) quasi-momentum of the free carriers.

When the modulation results from a single pump pulse (of the duration τ_M), at its tail end

$$f_M(\mathbf{p}, \mathbf{r}; \tau_M \lesssim t \ll \tau_0) \simeq f_0(\mathbf{p} - \mathbf{p}_0(\mathbf{r})), \quad (10)$$

while in its wake ($t > \tau_M$)

$$f_M(\mathbf{p}, \mathbf{r}; t > \tau_M) \simeq (f_0(\mathbf{p} - \mathbf{p}_0(\mathbf{r})) - f_0(\mathbf{p})) e^{-t/\tau_0} + f_0(\mathbf{p}), \quad (11)$$

where

$$\mathbf{p}_0(\mathbf{r}) = e \int_{-\infty}^{\infty} \mathbf{E}_M(\mathbf{r}, t') dt' \quad (12)$$

is the total impulse transferred to a free electron from the pump pulse.

In particular, for the Gaussian pump pulse

$$\mathbf{E}_M(t) = E_0 e^{-t^2/\tau_M^2} \cos(\omega_M t), \quad (13)$$

we find

$$p_0 = eE_0\tau_M \sqrt{\pi} e^{-\omega_M^2\tau_M^2/4}, \quad (14)$$

controlled by the product $\omega_M\tau_M/\pi$, which defines the number of significant cycles in the rapidly decaying pulse. For an ultra-short pump pulse ($\omega_M\tau_M < \pi$), the impulse $p_0 \simeq eE_0\tau_M$ for a doped semiconductor under typical experimental conditions can become of the order of the Fermi momentum p_F . On the other hand, for $\omega_M\tau_M > \pi$, due to the cancellation between positive and negative regions of $E_M(t)$ the drift momentum p_0 becomes exponentially small – so that the pump pulse takes the free electrons to a strongly non-equilibrium state but then, reversibly, brings them back close to the equilibrium. It was the latter regime that was recently investigated in the experiments of Ref. [20], where the pump pulse had roughly three significant cycles.

The Carrier Drift Modulation approach, that we introduced in the present work, corresponds to the case $\omega_M\tau_M < \pi$, when the pump, almost instantaneously on free carrier time scale, creates a new, anisotropic medium with drifting electrons.

Prior to the action of the pump in this setting, the probe wave is a superposition of the conventional transverse plasmons with the dispersion relation

$$\omega = \sqrt{\omega_p^2 + k^2 c^2/\epsilon_\infty}, \quad (15)$$

where ϵ_∞ is the lattice contribution to the dielectric permittivity and k is the wavenumber. At the moment of the arrival of an abrupt Carrier Drift Modulation, the dispersion relation of the probe waves evolves into

$$\omega' = \sqrt{\omega_p^2 - \Omega^2 + k^2 c^2/\epsilon_\infty}, \quad (16)$$

where the correction Ω depends on the acquired drift momentum p_0 and the free carrier dispersion non-parabolicity. However, in order to satisfy the boundary conditions at the temporary interface induced by the arrival of the modulation pulse, the probe field must also acquire components propagating in the directions opposite to those of the original wave. Both of these time-refracted and time-reflected components now oscillate at the new frequency ω' , with the time-refraction and time-reflection amplitudes that scale as

$$\mathcal{T} \simeq \frac{\omega + \omega'}{2\omega}, \quad \mathcal{R} \simeq \frac{\omega - \omega'}{2\omega} \quad (17)$$

in the limit of small loss $\omega\tau_0 \gg 1$. The detailed analysis of the time-reflection and time-refraction in a drift-modulated medium will be presented in section V.

Most importantly, the proposed Carrier Drift Modulation opens the route to the Hyperbolic Time Crystal, where the optical modulation not only turns an isotropic semiconductor into a hyperbolic medium, but at the same time also reduces its absorption via the mechanism of parametric amplification.

III. THE WAVE EQUATION FOR CARRIER DRIFT MODULATION

Here, we consider the electromagnetic response of an isotropic conducting medium under the Carrier Drift Modulation, introduced in the previous section. For a probe field $\mathbf{E}(\mathbf{r}, t)$ that is much smaller than the peak amplitude of the pump pulse E_M , the resulting linear response can be described by the linearized kinetic equation [18]

$$\frac{\partial g}{\partial t} + \mathbf{v}_p \cdot \nabla g + e\mathbf{E} \cdot \frac{\partial f_M}{\partial \mathbf{p}} + e\mathbf{E}_M \cdot \frac{\partial g}{\partial \mathbf{p}} = -\frac{g}{\tau_0}, \quad (18)$$

where the complete distribution function

$$f(\mathbf{p}, \mathbf{r}; t) = f_M(\mathbf{p}; t) + g(\mathbf{p}, \mathbf{r}; t). \quad (19)$$

With the free carriers Fermi velocity $v_F \ll c$, the effects of spatial dispersion that originate from the second term at the right-hand side of Eqn. (18) can be neglected, and we obtain

$$g = - \int_{-\infty}^t dt' e\mathbf{E}(\mathbf{r}, t') \cdot \frac{f_M(\mathbf{p} - \mathbf{p}_M(\mathbf{r}, t) + \mathbf{p}_M(\mathbf{r}, t'); t')}{\partial \mathbf{p}} \times \exp\left(-\frac{t - t'}{\tau_0}\right). \quad (20)$$

Substituting (7) into (20), we obtain

$$g = -\frac{e^{-t/\tau_0}}{\tau_0} \int_{-\infty}^t dt' \int_{-\infty}^{t'} dt'' e^{t''/\tau_0} \times e\mathbf{E}(\mathbf{r}, t') \cdot \frac{\partial f_0(\mathbf{p} - \mathbf{p}_M(\mathbf{r}, t) + \mathbf{p}_M(\mathbf{r}, t''))}{\partial \mathbf{p}}, \quad (21)$$

Substituting into Maxwell's Equations the free current density defined by the distribution function $g(\mathbf{p}, \mathbf{r}; t)$ from Eqn. (18), we obtain the Wave Equation (see Appendix A)

$$\begin{aligned} & \left(\frac{\partial}{\partial t} + \frac{1}{\tau_0} \right) \left(\frac{\partial^2 \mathbf{E}}{\partial t^2} + \frac{c^2}{\epsilon_\infty} \operatorname{curl} \operatorname{curl} \mathbf{E} \right) + \omega_p^2 \frac{\partial \mathbf{E}}{\partial t} \\ & = \frac{\partial}{\partial t} \left[\mathbf{M}_0 \cdot \mathbf{E} + e^{-\frac{t}{\tau_0}} \int_{-\infty}^t dt' \frac{\partial \mathbf{M}}{\partial t} \cdot \mathbf{E}(t') \right], \end{aligned} \quad (22)$$

where the plasma frequency

$$\omega_p^2 = \frac{4\pi n_0 e^2}{m_* \epsilon_\infty}, \quad (23)$$

the modulation kernel

$$\begin{aligned} \mathbf{M}(t, t') & \equiv \omega_p^2 \int_{-\infty}^{t'} \frac{dt''}{\tau_0} \exp\left(\frac{t''}{\tau_0}\right) \\ & \times \left(1 - \frac{m_*}{\mathbf{m}[\mathbf{p}_M(t) - \mathbf{p}_M(t'')]} \right), \end{aligned} \quad (24)$$

and

$$\mathbf{M}_0(t) \equiv \mathbf{M}(t, t) e^{-\frac{t}{\tau_0}}. \quad (25)$$

Here, the modulated effective mass tensor

$$\frac{1}{m_{\alpha\beta}[\mathbf{q}]} = \left\langle \frac{\partial^2 \varepsilon_{\mathbf{p}+\mathbf{q}}}{\partial p_\alpha \partial p_\beta} \right\rangle_{\mathbf{p}} \quad (26)$$

with the phase space average defined as

$$\left\langle F[\mathbf{p} + \mathbf{q}] \right\rangle_{\mathbf{p}} \equiv \frac{\int d\mathbf{p} F(\mathbf{p} + \mathbf{q}) f_0(\mathbf{p})}{\int d\mathbf{p} f_0(\mathbf{p})}. \quad (27)$$

For a parabolic band

$$\left\langle \frac{\partial^2 \varepsilon_{\mathbf{p}+\mathbf{q}}}{\partial p_\alpha \partial p_\beta} \right\rangle_{\mathbf{p}} = \left\langle \frac{\partial^2 \varepsilon_{\mathbf{p}}}{\partial p_\alpha \partial p_\beta} \right\rangle_{\mathbf{p}} = \frac{\delta_{\alpha\beta}}{m_*} \quad (28)$$

is defined by the average effective mass m_* , so that $\mathbf{M} = 0$, the wave equation does not depend on the pump, and the modulation has no effect on the free carrier response to the probe field.

However, substantial electronic non-parabolicity is inherent to the conducting materials used in electro-optics, such as transparent conducting oxides [21, 22] and semiconductors [23]. Furthermore, this is generally not a small effect [24, 25]: e.g., over the range of relevant quasi-momenta the effective mass varies by $\sim 30\%$ in gallium arsenide [26–28] and by a factor of 5 in indium arsenide [26, 29].

The general wave equation (22) can be further simplified when the duration of the modulation pulse is smaller than the time scale of a single electromagnetic cycle of the signal $\mathbf{E}(\mathbf{r}, t)$, which reduces (22) to

$$\begin{aligned} & \left(\frac{\partial}{\partial t} + \frac{1}{\tau_0} \right) \left(\frac{\partial^2 \mathbf{E}}{\partial t^2} + \frac{c^2}{\epsilon_\infty} \operatorname{curl} \operatorname{curl} \mathbf{E} \right) + \omega_p^2 \frac{\partial \mathbf{E}}{\partial t} \\ &= \mathbf{M}_0 \cdot \left(\frac{\partial}{\partial t} - \frac{1}{\tau_0} \right) \mathbf{E}. \end{aligned} \quad (29)$$

In this approach (see Appendix B), the effect of the drift modulation leading to an abrupt change of $\mathbf{M}(t, t')$, is described by *three* independent boundary conditions at the time of the “temporal boundary” induced by the pump pulse. These boundary conditions correspond to the continuity of the fields

- (i) \mathbf{E} ,
- (ii) \mathbf{F} , and
- (iii) $\partial \mathbf{F} / \partial t$,

where the temporal displacement field \mathbf{F} is defined as

$$\mathbf{F} \equiv \frac{\partial \mathbf{E}}{\partial t} - e^{-\frac{t}{\tau_0}} \int_{-\infty}^t dt' \mathbf{M}(t, t') \cdot \mathbf{E}(\mathbf{r}, t'). \quad (30)$$

When the electronic relaxation time τ_0 is much larger than other characteristic time scale of the system dynamics (such as e.g., the modulation pulse duration τ_M , the signal period $2\pi/\omega$, and the time interval T_M between different modulation pulses), the drift modulation wave equation can be reduced to (see Appendix C)

$$\begin{aligned} & \frac{\partial^2 \mathbf{E}}{\partial t^2} + \frac{c^2}{\epsilon_\infty} \operatorname{curl} \operatorname{curl} \mathbf{E} + \frac{m_* \omega_p^2}{\mathbf{m}_M(t)} \mathbf{E} \\ &= \omega_p^2 m_* \frac{d\mathbf{m}^{-1}}{dt} \int_{-\infty}^t dt' \mathbf{E}(t'). \end{aligned} \quad (31)$$

where the time-dependent effective mass tensor

$$\frac{1}{\mathbf{m}_M} \equiv \frac{1}{\mathbf{m}[\mathbf{p}_M(t)]}. \quad (32)$$

Furthermore, when the duration of the modulation pulse is smaller than the time scale of a single electromagnetic cycle of the signal, Eqn. (31) reduces to

$$\frac{\partial^2 \mathbf{E}}{\partial t^2} + \frac{c^2}{\epsilon_\infty} \operatorname{curl} \operatorname{curl} \mathbf{E} + \omega_p^2 \frac{m_*}{\mathbf{m}_M} \mathbf{E} = 0. \quad (33)$$

with the continuity of the electric field $\mathbf{E}(\mathbf{r}, t)$ and the temporal displacement

$$\mathbf{F} = \frac{\partial \mathbf{E}}{\partial t} + \omega_p^2 \frac{m_*}{\mathbf{m}_M} \cdot \int_{-\infty}^t dt' \mathbf{E}(t'). \quad (34)$$

The general wave equation derived in the present section, that is applicable to general modulation field $\mathbf{E}_M(\mathbf{r}, t)$ in an arbitrary geometry, is one of the main results of the present work.

IV. THE DIELECTRIC PERMITTIVITY UNDER CARRIER DRIFT MODULATION

For a monochromatic probe field

$$\mathbf{E}(\mathbf{r}, t) = \mathbf{E}_\omega(\mathbf{r}) \exp(-i\omega t), \quad (35)$$

the free carriers polarization

$$\begin{aligned} \mathbf{P}(\mathbf{r}, t) &= \int_{-\infty}^t dt' \mathbf{j}(\mathbf{r}, t') \\ &= -\frac{\epsilon_\infty}{4\pi} \left[\frac{\omega_p^2}{\omega(\omega + \frac{i}{\tau_0})} + e^{-\frac{t}{\tau_0}} \int_{-\infty}^t dt' e^{(i\omega + \frac{1}{\tau_0})(t-t')} \right. \\ &\quad \left. \times \int_{-\infty}^{t'} dt'' e^{i\omega(t'-t'')} \mathbf{M}(t', t'') \right] \mathbf{E}(\mathbf{r}, t) \end{aligned} \quad (36)$$

The main contributions to the time integrals in (36) come from the intervals $0 < t - t' < 1/\omega$ and $0 < t' - t'' < 1/\omega$. If, and only if, the time that elapsed from the most recent *past* temporal boundary, is much larger than the oscillation period at the probe frequency, $2\pi/\omega$, the free carrier polarization can be expressed as

$$\mathbf{P}(t) = -\frac{\epsilon_\infty}{4\pi} \left[\frac{\omega_p^2}{\omega(\omega + \frac{i}{\tau_0})} - \frac{\mathbf{M}_0(t)}{\omega(\omega - \frac{i}{\tau_0})} \right] \mathbf{E}(t), \quad (37)$$

with

$$\mathbf{M}_0(t) = \omega_p^2 \sum_{t_n < t} e^{-\frac{t-t_n}{\tau_0}} \left(\frac{m_*}{\mathbf{m}[\Delta \mathbf{p}_n]} - \frac{m_*}{\mathbf{m}[\Delta \mathbf{p}_{n-1}]} \right), \quad (38)$$

where

$$\Delta \mathbf{p}_n \equiv \mathbf{p}_M(t) - \mathbf{p}_M\left(\frac{t_n + t_{n-1}}{2}\right) \quad (39)$$

is the difference between the drift momenta imposed by different modulation pulses.

We can therefore introduce the (time-dependent) dielectric permittivity tensor ϵ such that

$$\mathbf{D} \equiv \epsilon_\infty \mathbf{E} + 4\pi \mathbf{P} = \epsilon \cdot \mathbf{E}, \quad (40)$$

where

$$\begin{aligned} \epsilon_{\alpha\beta}(\omega; t) &= \epsilon_\infty \left(1 - \frac{\omega_p^2}{\omega(\omega + i/\tau_0)} \right) \delta_{\alpha\beta} \\ &+ \epsilon_\infty \frac{\Omega_{\alpha\beta}^2(t)}{\omega(\omega - i/\tau_0)}, \end{aligned} \quad (41)$$

and

$$\Omega_{\alpha\beta}^2 = \omega_p^2 \sum_{t_n < t} e^{-\frac{t-t_n}{\tau_0}} \left(\delta_{\alpha\beta} - m_* \left\langle \frac{\partial^2 \epsilon_{\mathbf{p}+\Delta\mathbf{p}_n}}{\partial p_\alpha \partial p_\beta} \right\rangle_{\mathbf{p}} \right). \quad (42)$$

In the limit of moderate carrier drift modulation ($\Delta p < p_F$), we find (see Appendix D)

$$\Omega_{\parallel}^2(t) \simeq 3 \frac{\alpha_* \omega_p^2}{m_0} \sum_{t_n < t} \Delta p_n^2 e^{-\frac{t-t_n}{\tau_0}}, \quad (43)$$

$$\Omega_{\perp}^2(t) \simeq \frac{\alpha_* \omega_p^2}{m_0} \sum_{t_n < t} \Delta p_n^2 e^{-\frac{t-t_n}{\tau_0}}, \quad (44)$$

where the Kane's non-parabolicity parameter α_* is on the order of the inverse bandgap energy E_g [30], and the subscripts correspond to the directions parallel (\parallel) and perpendicular (\perp) to the *pump* field \mathbf{E}_M modulating the material.

Therefore, in the wake of a single modulation pulse applied at $t = 0$, when $\tau_M \ll t \ll \tau_0$, the dielectric permittivity tensor of the drift-modulated isotropic medium takes the form

$$\epsilon_{\parallel, \perp} = \epsilon_\infty \left(1 - \frac{\omega_p^2 - \Omega_{\parallel, \perp}^2}{\omega^2} \right), \quad (45)$$

and describes hyperbolic response in the frequency band

$$\sqrt{\omega_p^2 - \Omega_{\parallel}^2} < \omega < \sqrt{\omega_p^2 - \Omega_{\perp}^2}. \quad (46)$$

Note however, that under the conditions of the carrier drift modulation, the time-dependent dielectric permittivity can only be introduced at the time that is at least several probe cycles after a temporary interface.

V. TEMPORAL REFLECTION

In its conventional setup, the temporal reflection occurs when the electromagnetic properties of a medium (such as its permittivity) change suddenly in time, while remaining uniform in space. This abrupt temporal discontinuity causes part of the wave to reflect – not spatially, but temporally. Here we consider the temporal

reflection that arises from the carrier drift modulation in an isotropic conducting material.

To avoid the complexity of the retardation of the pump pulse as it propagates through the medium, we consider the geometry of a subwavelength waveguide with metallic cladding that is transparent to the pump (supported by the bandwidth that is well above the plasma frequency of the cladding) – see Fig. 1. For a practical implementation, such system can be realized using a doped semiconductor waveguide (with the plasma frequency in mid-to far-infrared), with a thin conducting oxide cladding (such as e.g., indium tin oxide with the plasma wavelength close to the telecom band around 1.55 μm).

We consider a guided wave, that was propagating at the frequency $\omega > \omega_p$ before the onset of the modulation ($t < 0$). For the wave equation (29) this corresponds to $\mathbf{M} = 0$, leading to the “incident” wave

$$\mathbf{E}_i(\mathbf{r}, t) = \mathbf{E}_0(\mathbf{r}) \exp(-i\omega t), \quad (47)$$

in the geometry of Fig. 1, where

$$\mathbf{E}_0(\mathbf{r}) = E_0 \mathbf{f}(k_z z) e^{ik_x x + ik_y y} \quad (48)$$

and

$$\omega = kc/\sqrt{\epsilon_\omega}, \quad (49)$$

with the dielectric permittivity ϵ_ω defined by Eqn. (45) with $\Omega_{\alpha\beta}$ set to zero. Note that due to the presence of the electromagnetic absorption that is inherent to conducting materials, at least one of the quantities k or ω in Eqns. (47), (49) has a nonzero imaginary part.

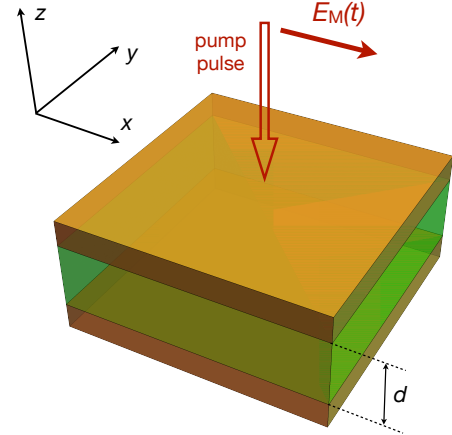


FIG. 1. Schematic of the waveguide geometry under drift modulation. The waveguide core consists of a conducting material with plasma frequency ω_p , chosen to be comparable to the probe (signal) frequency ω . The cladding behaves as a metal at the signal wavelength while remaining partially transparent to the high-frequency optical pump pulse. The pump is polarized within the plane of the waveguide, and the signal propagates in the transverse electromagnetic (TEM) mode of the structure.

When the waveguide thickness d (see Fig. 1) is well below the wavelength at the signal frequency, the only propagating mode in the system is the so called TEM-wave [31] with the electric field that is perpendicular to the waveguide plane and only depends on the in-plane coordinates:

$$\mathbf{f}_{\text{TEM}} = \hat{\mathbf{z}}, \quad k_z = 0. \quad (50)$$

For the TEM-polarized field, when the pump pulse duration τ_M is much shorter than the modulation interval T_M and the free carrier relaxation time τ_0 , from Eqns. (24),(25) we find

$$\mathbf{M}(t, t') = \hat{\mathbf{z}} \hat{\mathbf{z}} \theta(t) \exp\left(\frac{\min[t', 0]}{\tau_0}\right) \Omega_{\perp}^2, \quad (51)$$

$$\mathbf{M}_0(t) = \hat{\mathbf{z}} \hat{\mathbf{z}} \theta(t) \exp\left(-\frac{t}{\tau_0}\right) \Omega_{\perp}^2, \quad (52)$$

where (see Fig. 1)

$$\Omega_{\perp}^2 = \omega_p^2 \left(1 - m_* \left\langle \frac{\partial^2 \epsilon_{\mathbf{p} + \hat{\mathbf{x}} p_0}}{\partial p_z^2} \right\rangle_{\mathbf{p}}\right) \simeq \frac{4}{3} \frac{\alpha_* p_0^2}{m_0} \omega_p^2, \quad (53)$$

$\theta(t)$ is the Heaviside's function, and \mathbf{p}_0 was defined in Eqn. (12).

For the TEM-polarized field at $0 < t \ll \tau_0$, we then obtain

$$\mathbf{E} = \hat{\mathbf{z}} e^{ik_x x + ik_y y} \sum_{m=1}^3 s_m \exp(-i\omega_m t), \quad (54)$$

where the frequencies ω_m are the three solutions of the cubic equation

$$\begin{aligned} \omega^3 + \frac{i}{\tau_0} \omega^2 - \left(\omega_p^2 - \Omega_{\perp}^2 + \frac{k^2 c^2}{\epsilon_{\infty}}\right) \omega \\ = \frac{i}{\tau_0} \left(\Omega_{\perp}^2 + \frac{k^2 c^2}{\epsilon_{\infty}}\right), \end{aligned} \quad (55)$$

which can be equivalently expressed in the form

$$\omega = \frac{kc}{\sqrt{\epsilon_{\perp}^{\text{eff}}(\omega)}}, \quad (56)$$

where the effective transverse permittivity

$$\epsilon_{\perp}^{\text{eff}}(\omega) \equiv \epsilon_{\infty} \left(1 - \frac{\omega_p^2 - \Omega_{\perp}^2 \left(1 - \frac{i}{\omega \tau_0}\right)}{\omega \left(\omega + \frac{i}{\tau_0}\right)}\right) \quad (57)$$

is consistent with ϵ_{\perp} in Eqn. (45).

For a relatively small loss, when $c \tau_0 \gg 1/k$ [32], we find

$$\omega_{1,2} = \pm \omega' - i \frac{\gamma}{\tau_0}, \quad (58)$$

$$\omega_3 = -i \frac{1 - 2\gamma}{\tau_0} \quad (59)$$

where the new frequency

$$\omega' = \sqrt{\omega_p^2 - \Omega_{\perp}^2 + k^2 c^2 / \epsilon_{\infty}}, \quad (60)$$

and the dimensionless extinction rate

$$\gamma = \frac{1}{2} \frac{\omega_p^2 - 2\Omega_{\perp}^2}{\omega_p^2 - \Omega_{\perp}^2 + k^2 c^2 / \epsilon_{\infty}}. \quad (61)$$

Therefore, in the electric field (54) the amplitudes s_1 and s_2 correspond to the time-transmission and time-reflection coefficients \mathcal{R} and \mathcal{T} , while s_3 accounts for the amplitude of the time-evanescent wave \mathcal{S} – which yields

$$\begin{aligned} \mathbf{E}(\mathbf{r}, t > 0) = E_0 \mathbf{f}_{\text{TEM}} \left\{ e^{-\frac{\gamma}{\tau_0} t + i\mathbf{k} \cdot \mathbf{r}} \left[\mathcal{T} e^{-i\omega' t} + \mathcal{R} e^{i\omega' t} \right] \right. \\ \left. + e^{-\frac{1-2\gamma}{\tau_0} t + i\mathbf{k} \cdot \mathbf{r}} \mathcal{S} \right\}, \end{aligned} \quad (62)$$

where $\mathbf{r} \equiv (x, y)$.

From the continuity of the fields \mathbf{E} , \mathbf{F} and $\partial\mathbf{F}/\partial t$ at the temporal interface $t = 0$, we obtain (see Appendix E):

$$\mathcal{R} = \frac{\eta_{\omega} \omega (\omega - \omega' + i \frac{1-\gamma}{\tau_0}) - i \frac{1-2\gamma}{\tau_0} (\omega' - i \frac{\gamma}{\tau_0})}{2 \omega' \left(\omega' - i \frac{1-3\gamma}{\tau_0}\right)}, \quad (63)$$

$$\mathcal{T} = \frac{\eta_{\omega} \omega (\omega + \omega' + i \frac{1-\gamma}{\tau_0}) + i \frac{1-2\gamma}{\tau_0} (\omega' + i \frac{\gamma}{\tau_0})}{2 \omega' \left(\omega' + i \frac{1-3\gamma}{\tau_0}\right)}, \quad (64)$$

$$\mathcal{S} = \frac{\omega'^2 - \eta_{\omega} \omega (\omega + 2i\gamma/\tau_0) + \gamma^2/\tau_0^2}{\omega'^2 + (1 - 3\gamma)^2/\tau_0^2}, \quad (65)$$

In the low-loss limit $\omega \tau_0 \gg 1$ we find

$$\omega' \rightarrow \sqrt{\omega^2 - \Omega_{\perp}^2} \rightarrow \sqrt{\eta_{\omega}} \omega, \quad (66)$$

so that

$$\mathcal{R} \simeq \frac{\eta_{\omega} \omega (\omega - \omega')}{2 \omega'^2} \rightarrow \frac{\omega - \omega'}{2 \omega}, \quad (67)$$

$$\mathcal{T} \simeq \frac{\eta_{\omega} \omega (\omega + \omega')}{2 \omega'^2} \rightarrow \frac{\omega + \omega'}{2 \omega}, \quad (68)$$

$$\mathcal{S} \simeq \frac{\omega'^2 - \eta_{\omega} \omega^2}{\omega'^2} \rightarrow 0. \quad (69)$$

Note that the conventional approach [2, 3] based on the idea of a nearly-instantaneous change in the dielectric permittivity tensor in both time and frequency, can not reproduce the results of the present section, even in the lossless limit when the presence of the time-evanescent wave beyond the temporal interface can be neglected (see Eqn. (69)). Since the drift modulation rapidly changes the *current density*, the resulting dielectric polarization $\mathbf{P} \propto \int dt \mathbf{j}(t)$ remains *continuous* across the transition – which cannot be described by a step-like behavior of the time-dependent dielectric permittivity [2, 3].

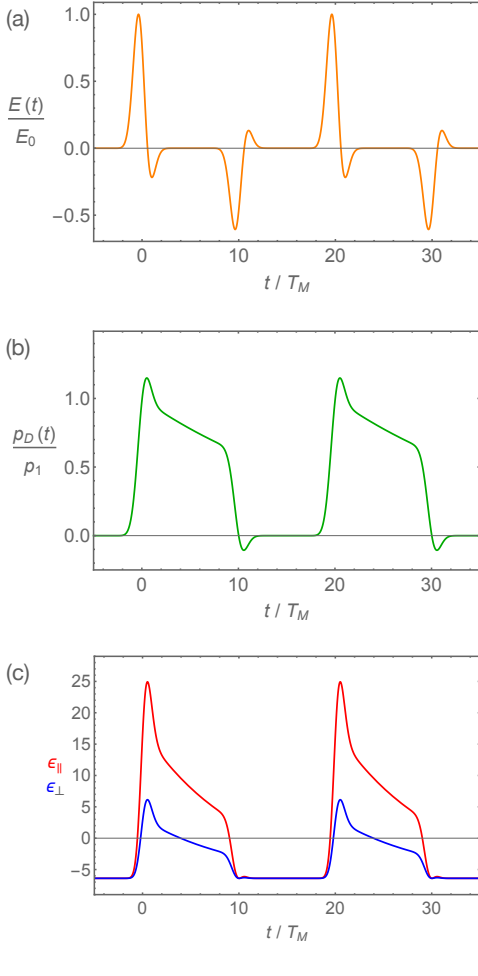


FIG. 2. Panel (a): Modulation pulse sequence used for hypercrystal drift modulation (see Eqns. (70),(71)). Note the nonzero average field for a single modulation pulse, and alternating signs of the pulse train. Panel (b): Drift momentum of the free carriers, calculated as the average over the free electron distribution. Note that the carrier drift momentum p_D is distinct from the pump impulse p_M . Panel (c): Time-dependent dielectric permittivity of the medium, obtained from the electrical displacement vector $\mathbf{D}(t)$ corresponding to the time-dependent distribution function of the free carriers $f(\mathbf{p}, t)$. The “parallel” (\parallel) and “perpendicular” (\perp) directions (shown by red and blue curves, respectively) are defined relative to the modulation field \mathbf{E}_M (see also Fig. 1). Numerical values used in the calculation correspond to a heavily doped gallium arsenide sample [23], with the relaxation time $\tau_0 = 0.1$ and the modulation interval $T_M = 20$ fs.

VI. THE HYPERBOLIC TIME CRYSTAL

With the distortion of the free electron velocity distribution in the direction of the electric field of the pump pulse, Carrier Drift Modulation creates a transient anisotropy in the free carrier electromagnetic response – see Eqn. (45). With the proper choice of the amplitude and phase for modulation pulse, coherent pulse train can

“imprint” the desired electron drift momentum profile $\mathbf{p}(t)$, as long as the time interval between the modulation pulses T_M is substantially smaller than the electron scattering time τ_0 . In particular, the “binary phase-shift keying” modulation sequence,

$$\mathbf{E}_M(t) = \sum_n [\mathbf{E}_1(t - 2nT_M) - e^{-T_M/\tau_0} \mathbf{E}_1(t - (2n-1)T_M)], \quad (70)$$

or, in the limit $\tau_0 \ll T_M$

$$\mathbf{E}_M(t) = \sum_n (-1)^n \mathbf{E}_1(t - nT_M), \quad (71)$$

where $\mathbf{E}_1(t)$ is a single ultra-fast optical pulse, will lead to the “on-off” drift momentum modulation – see Fig. 2.

With the relatively low absorption in the original isotropic material at the probe/signal frequency ω ,

$$\omega\tau_0 \gg 1, \quad (72)$$

when the signal is injected into the system after it already reached the modulated steady state, the photonic time crystal defined by the Carrier Drift Modulation (71) operates as a temporal metamaterial when $\omega T_M \ll 1$, and as the time hypercrystal for $\omega T_M \gtrsim 1$.

Signal propagation in the temporal metamaterial regime is described by the standard wave equation with the effective dielectric permittivity tensor

$$\epsilon_{\parallel,\perp} = \epsilon_\infty \left(1 - \frac{\omega_p^2 - \langle \Omega_{\parallel,\perp}^2 \rangle}{\omega(\omega + i/\tau_0)} \right). \quad (73)$$

where $\langle \dots \rangle$ represents the time average over a full period of the modulation pulse train (e.g., $2T_M$ for the binary phase-shift protocol of Eqn. (71)), with the hyperbolic response in the signal frequency band

$$\sqrt{\omega_p^2 - \langle \Omega_{\parallel}^2 \rangle} < \omega < \sqrt{\omega_p^2 - \langle \Omega_{\perp}^2 \rangle}. \quad (74)$$

The temporal hypercrystal regime (defined by the requirement $\omega T_M \gtrsim 1$) offers the temporal analogue of the “spatial hypercrystals” [33], the composites with the unit cell that contains both hyperbolic media and natural materials. Similar to the hyperbolic material, the hypercrystal also supports propagating fields with the wavenumbers that are unlimited by the signal frequency, albeit with a nontrivial bandstructure and multiple bandgaps.

However, with the proper choice of the signal frequency ($\omega T_M = \pi$), carrier drift modulation now satisfies the standard requirement for the parametric amplification [34] – leading to the effective signal gain in the drift-modulated medium. With the general high-efficiency of the parametric amplification processes that turned the corresponding devices into the workhorses of high-bandwidth electronics [35], the parametric gain in the time hypercrystal can reach to the level of the signal absorption in the original (unmodulated) conducting

medium – which offers, for the first time, the possibility of a lossless hyperbolic medium.

At the length scales relevant for high-wavenumber fields propagating in a hyperbolic medium, the spatial variation of the pump pulse can be neglected, so to avoid dealing with the pump retardation we are no longer limited to the waveguide geometry of the previous section. Furthermore, with the signal / probe primarily supported by the high wavenumbers $k \gg \omega/c$, its propagation can be described within the framework of the quasistatic limit [36], where the electric field is defined by the scalar potential

$$\mathbf{E} = -\nabla\phi. \quad (75)$$

For the wave equation in the quasistatic limit we obtain (see Appendix G)

$$\begin{aligned} \frac{d^2\phi_{\mathbf{k}}}{dt^2} + \frac{1}{\tau_0} \frac{d\phi_{\mathbf{k}}}{dt} + \left(\omega_p^2 - \mathcal{M}_{\mathbf{k}}^{(0)}(t) \right) \phi_{\mathbf{k}} \\ = e^{-\frac{t}{\tau_0}} \int_{-\infty}^t dt' \frac{\partial \mathcal{M}_{\mathbf{k}}}{\partial t'} \phi_{\mathbf{k}}(t'), \end{aligned} \quad (76)$$

where the (scalar) modulation kernel $\mathcal{M}_{\mathbf{k}}(t)$ is given by

$$\mathcal{M}_{\mathbf{k}}(t, t') = \frac{\mathbf{k} \cdot \mathbf{M}(t, t') \cdot \mathbf{k}}{k^2}, \quad (77)$$

and

$$\mathcal{M}_{\mathbf{k}}^{(0)}(t) \equiv e^{-\frac{t}{\tau_0}} \mathcal{M}_{\mathbf{k}}(t, t) \quad (78)$$

When the duration of the modulation pulse is smaller than the time scale of a single electromagnetic cycle of the signal, Eqn. (76) can be reduced to

$$\frac{d^2\phi_{\mathbf{k}}}{dt^2} + \frac{1}{\tau_0} \frac{d\phi_{\mathbf{k}}}{dt} + \left(\omega_p^2 - \mathcal{M}_{\mathbf{k}}^{(0)}(t) \right) \phi_{\mathbf{k}} = 0, \quad (79)$$

with the boundary conditions at the time of each modulation pulse corresponding to the continuity of the (i) scalar potential ϕ and (ii) the auxiliary time displacement potential

$$\psi(\mathbf{r}, t) \equiv \frac{\partial\phi}{\partial t} - e^{-\frac{t}{\tau_0}} \int_{-\infty}^t dt' \mathcal{M}_{\mathbf{k}}(t, t') \cdot \phi(\mathbf{r}, t'). \quad (80)$$

Neglecting the material absorption ($\omega\tau_0 \rightarrow \infty$), for the “on-off” carrier drift modulation of Eqns. (70),(71),

$$\mathcal{M}_{\mathbf{k}}^{(0)} = \begin{cases} \xi_{\mathbf{k}}, & \lfloor t/T_M \rfloor = 2n, \\ 0, & \lfloor t/T_M \rfloor = 2n+1, \end{cases} \quad (81)$$

where n is an integer, $\lfloor x \rfloor$ represents the integer part of x , and

$$\xi_{\mathbf{k}} = \frac{k_{\parallel}^2}{k^2} \frac{\Omega_{\parallel}^2}{\omega_p^2} + \frac{k_{\perp}^2}{k^2} \frac{\Omega_{\perp}^2}{\omega_p^2}, \quad (82)$$

with the components \mathbf{k}_{\parallel} and \mathbf{k}_{\perp} parallel and perpendicular to the modulation pulse field \mathbf{E}_1 . Here

$$\Omega_{\parallel}^2 = \frac{\alpha_* p_1^2}{m_0} \omega_p^2, \quad (83)$$

$$\Omega_{\perp}^2 = \frac{\alpha_* p_1^2}{m_0} \omega_p^2, \quad (84)$$

and p_1 is the transferred impulse from a single modulation pulse in (70), (71):

$$\mathbf{p}_1 \equiv \int_{-\infty}^{\infty} dt e \mathbf{E}_1(t), \quad (85)$$

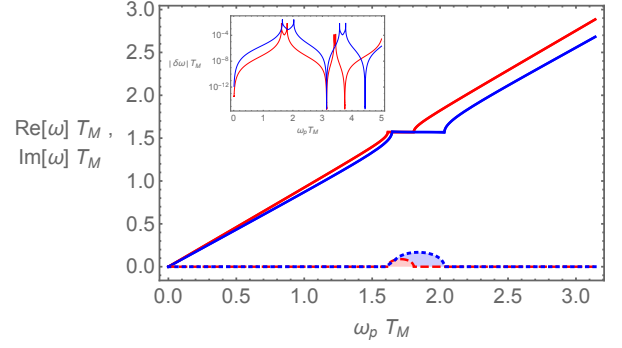


FIG. 3. Floquet–Bloch frequency in the drift-modulated hypercrystal, shown as a function of the product of the material plasma frequency and the modulation interval for $\xi_{\mathbf{k}} = 0.3$ (red lines) and $\xi_{\mathbf{k}} = 0.5$ (blue curves). Solid and dashed lines represent the real and imaginary parts of the Floquet–Bloch frequency, respectively. The results of the exact solution (88) and its analytical approximation (90), (91) are indistinguishable in the main plot, with the small ($\lesssim 10^{-4}$) difference between the exact and analytical solutions shown in the inset.

For the Floquet-Bloch states in the resulting time crystal,f

$$\mathbf{E}(\mathbf{r}, t) = \mathbf{u}(t) e^{i\mathbf{k} \cdot \mathbf{r} - i\omega t}, \quad (86)$$

with

$$\mathbf{u}(t) = \mathbf{u}(t + 2T_M), \quad (87)$$

we obtain

$$\begin{aligned} \cos[2\omega T_M] &= \cos[\omega_p T_M] \cos[\omega_{\mathbf{k}} T_M] \\ &- \frac{1}{2} \left(\frac{\omega_{\mathbf{k}}}{\omega_p} + \frac{\omega_p}{\omega_{\mathbf{k}}} \right) \sin[\omega_p T_M] \sin[\omega_{\mathbf{k}} T_M], \end{aligned} \quad (88)$$

where

$$\omega_{\mathbf{k}} \equiv \sqrt{\omega_p^2 - (k_{\parallel}/k)^2 \Omega_{\parallel}^2 - (k_{\perp}/k)^2 \Omega_{\perp}^2}. \quad (89)$$

An accurate solution of Eqn. (88) can be expressed as

$$\begin{aligned} \text{Re}[\omega] &= \frac{\omega_p + \omega_k}{2} + \frac{1}{T_M} \tan[(\omega_p + \omega_k) T_M] \\ &\times \text{Re} \sqrt{1 + \frac{\left(\sqrt{\frac{\omega_k}{\omega_p}} - \sqrt{\frac{\omega_p}{\omega_k}}\right)^2 \sin[\omega_p T_M] \sin[\omega_k T_M]}{\sin[(\omega_p + \omega_k) T_M] \tan[(\omega_p + \omega_k) T_M]}} \\ &- \frac{1}{T_M} \tan[(\omega_p + \omega_k) T_M] \end{aligned} \quad (90)$$

and

$$\begin{aligned} \text{Im}[\omega] &= \text{Im} \frac{1}{T_M} \left[\tan^2[(\omega_p + \omega_k) T_M] \right. \\ &+ \left. \left(\sqrt{\frac{\omega_k}{\omega_p}} - \sqrt{\frac{\omega_p}{\omega_k}} \right)^2 \frac{\sin[\omega_p T_M] \sin[\omega_k T_M]}{\cos[(\omega_p + \omega_k) T_M]} \right]^{1/2}. \end{aligned} \quad (91)$$

In Fig. 3 we show the exact solution of Eqn. (88), with absolute error of the analytical expressions (90), (91) in its inset.

In the time metamaterial regime $\omega_p T_M \ll 1$, Eqn. (88) reduces to

$$\omega^2 = \left(1 - \frac{\xi_k}{2}\right) \omega_p^2. \quad (92)$$

Substituting (82) into (92), we obtain the standard effective medium dispersion

$$\epsilon_{\parallel} k_{\parallel}^2 + \epsilon_{\perp} k_{\perp}^2 = 0, \quad (93)$$

where the effective permittivity tensor

$$\epsilon_{\parallel, \perp} = \epsilon_{\infty} \left(1 - \frac{\omega_p^2 - \frac{1}{2} \Omega_{\parallel}^2}{\omega^2}\right) \quad (94)$$

is consistent with (73). As expected, in the frequency range (46) the time metamaterial behaves as a hyperbolic medium.

In contrast to this behavior, when $\omega_p T_M \sim \pi n/2$ for any integer n , the photonic time crystal formed in the proposed drift modulation approach, shows bandgaps with $\text{Im}[\omega] > 0$. This corresponds to the photonic time crystal gain [9], whose physical origin lies in the optical parametric amplification due to the periodic optical modulation of the medium.

For a given material with its plasma frequency ω_p , the choice of the modulation interval T_M defines the interval of ξ_k with a nonzero gain – see Fig. 4(a). Naturally, due to a finite absorption in the system, it will primarily support the waves with the largest gain $\text{Rm}[\omega]$, and thus the smallest amount of attenuation. In Fig. 4(b) we show how the corresponding value ξ_k^{\max} varies with $\omega_p T_M$ (inset) and plot the resulting maximum gain as a function of ξ_k^{\max} .

From Eqn. (82), for a fixed value of ξ_k^{\max} we find

$$\left(\xi_k^{\max} - \frac{\Omega_{\parallel}^2}{\omega_p^2}\right) k_{\parallel}^2 + \left(\xi_k^{\max} - \frac{\Omega_{\perp}^2}{\omega_p^2}\right) k_{\perp}^2 = 0, \quad (95)$$

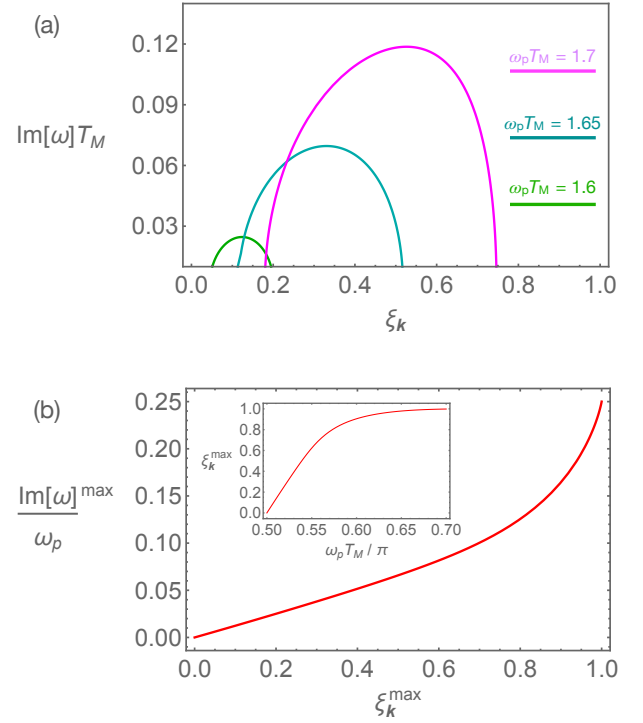


FIG. 4. Parametric gain in the photonic bandgap of the hyperbolic time crystal. Panel (a): Parametric gain as a function of ξ_k for different values of the product $\omega_p T_M$. Panel (b): Parametric gain as a function of ξ_k^{\max} , where ξ_k^{\max} is defined as the value of ξ_k corresponding to the maximum gain for a given value of $\omega_p T_M$. The inset shows the dependence of ξ_k^{\max} on $\omega_p T_M / \pi$.

which implies hyperbolic dispersion when

$$\frac{\Omega_{\perp}^2}{\omega_p^2} < \xi_k^{\max} < \frac{\Omega_{\parallel}^2}{\omega_p^2}, \quad (96)$$

or (see Eqns. (83), (84))

$$\frac{\alpha_* p_1^2}{m_0} < \xi_k^{\max} < 3 \frac{\alpha_* p_1^2}{m_0}. \quad (97)$$

With a continuous variation of ξ_k^{\max} as function of the modulation interval T_M (see the inset of Fig. 4(b)), the range (46) should be easily accessible in an experiment.

Furthermore, in highly doped semiconductors such as GaAs and InGaAs [23], the “quality factor” $\omega_p \tau_0 > 10$, so that the parametric gain in the hyperbolic time crystal (see Fig. 4(b)) can reach and even exceed the material absorption – making it possible to bring the dream of a lossless hyperbolic material to the reality of practical engineering.

VII. PRACTICAL CONSIDERATIONS

With the present stage of development in the field of low-loss optical materials with free charge carriers, highly

doped semiconductors and transparent conducting oxides (TCOs) can support the proposed approach of the carrier drift modulation, suitable respectively for mid- and near-infrared wavelength range. With $\omega_p \tau_0 \sim 5$ for TCOs [22] and $\omega_p \tau_0 > 10$ for doped semiconductors [23], the parametric gain in the time hypercrystal (see Fig. 4(b)) can overcome the material absorption in both of these platforms.

Furthermore, with the signal in the mid- or near-infrared frequency bands, using a few femtosecond pump pulse will satisfy the drift modulation requirement of $\tau_M \ll 2\pi/\omega$.

However, to reach the hyperbolic regime, the impulse p_1 transferred to the free electrons from the pump pulse (see the inequality (46)) must reach the values when

$$\frac{\alpha_* p_1^2}{m_0} \sim 0.1, \quad (98)$$

so that the peak amplitude of the pump pulse

$$E_M \sim \frac{p_1}{e\tau_M} \sim \sqrt{\frac{0.1m_0}{\alpha_* e^2 \tau_M^2}}, \quad (99)$$

For $\text{Ga}_{0.47}\text{In}_{0.53}\text{As}$ we find $m_0 = 0.41m_e$, where m_e is the electron mass, and $\alpha_* \simeq 1.35 \text{ eV}^{-1}$ [37], so that for $\tau_M \sim 3 \text{ fsec}$ we find $E_M \sim 500 \text{ kV/cm}$, which is several orders of magnitude below the peak amplitudes of $\sim 100 \text{ MV/cm}$ of commercial single-cycle IR sources [38].

The drift modulation approach introduced in the present work, therefore allows to induce a loss-free hyperbolic time crystal in an existing and well-established semiconductor material platform, using only commercially available sources.

VIII. CONCLUSIONS

In summary, we have introduced Carrier Drift Modulation, a novel mechanism for creating temporal boundaries and enabling the formation of photonic time crystals. This approach paves the way toward hyperbolic temporal metamaterials and hyperbolic time crystals, establishing a new paradigm in time-domain photonics. Importantly, we show that the very process responsible for forming the hyperbolic time crystal can simultaneously compensate intrinsic material losses in the supporting medium. Remarkably, such lossless hyperbolic time crystals can be realized using existing materials and readily available light sources, underscoring both the practicality and transformative potential of this concept.

IX. ACKNOWLEDGEMENTS

B.S. is grateful to Ohad Segal for useful discussions.

Appendix A: The Wave Equation

With the linear-response distribution function g given by Eqn. (18), for the corresponding current density we obtain

$$\mathbf{j} = \frac{n_0 e^2}{\tau_0} \int_{-\infty}^t dt' \int_{-\infty}^{t'} dt'' \exp\left(-\frac{t-t''}{\tau_0}\right) \times \frac{1}{\mathbf{m}[\mathbf{p}_M(\mathbf{r}, t) - \mathbf{p}_M(\mathbf{r}, t'')]} \cdot \mathbf{E}(\mathbf{r}, t'), \quad (A1)$$

where the modulated effective mass tensor

$$\frac{1}{m_{\alpha\beta}[\mathbf{q}]} = \left\langle \frac{\partial^2 \varepsilon_{\mathbf{p}+\mathbf{q}}}{\partial p_\alpha \partial p_\beta} \right\rangle_{\mathbf{p}} \quad (A2)$$

with the phase space average defined as

$$\left\langle F[\mathbf{p}+\mathbf{q}] \right\rangle_{\mathbf{p}} = \frac{\int d\mathbf{p} F(\mathbf{p}+\mathbf{q}) f_0(\mathbf{p})}{\int d\mathbf{p} f_0(\mathbf{p})}. \quad (A3)$$

Note that for a parabolic band

$$\left\langle \frac{\partial^2 \varepsilon_{\mathbf{p}+\mathbf{q}}}{\partial p_\alpha \partial p_\beta} \right\rangle_{\mathbf{p}} = \left\langle \frac{\partial^2 \varepsilon_{\mathbf{p}}}{\partial p_\alpha \partial p_\beta} \right\rangle_{\mathbf{p}} \equiv \frac{\delta_{\alpha\beta}}{m_*} \quad (A4)$$

is defined by the average effective mass m_* , so that the current density (A1) does not depend on the pump, and the modulation has no effect on the free carrier response to the probe field.

Introducing the modulation kernel

$$\mathbf{M}(t, t') \equiv \omega_p^2 \int_{-\infty}^{t'} \frac{dt''}{\tau_0} \exp\left(\frac{t''}{\tau_0}\right) \times \left(1 - \frac{m_*}{\mathbf{m}[\mathbf{p}_M(t) - \mathbf{p}_M(t'')]} \right), \quad (A5)$$

where the plasma frequency

$$\omega_p^2 = \frac{4\pi n_0 e^2}{m_* \epsilon_\infty}, \quad (A6)$$

and ϵ_∞ is the “background” dielectric permittivity from the crystal lattice, we obtain

$$\mathbf{j} = \frac{\epsilon_\infty \omega_p^2}{4\pi} \int_{-\infty}^t dt' e^{-\frac{t-t'}{\tau_0}} \mathbf{E}(\mathbf{r}, t') - \frac{\epsilon_\infty}{4\pi} e^{-\frac{t}{\tau_0}} \int_{-\infty}^t dt' \mathbf{M}(t, t') \cdot \mathbf{E}(\mathbf{r}, t'), \quad (A7)$$

Note that at the time scale when the electron relaxation can be neglected, the modulation kernel reduces to

$$\mathbf{M}(t, t') = \omega_p^2 \left(1 - \frac{m_*}{\mathbf{m}[\mathbf{p}_M(t)]}\right) \quad (A8)$$

In a non-magnetic medium, the evolution of the probe electric field $\mathbf{E}(\mathbf{r}, t)$ is defined by the wave equation

$$\epsilon_\infty \frac{\partial^2 \mathbf{E}}{\partial t^2} + c^2 \text{curl} \text{curl} \mathbf{E} + 4\pi \frac{\partial \mathbf{j}}{\partial t} = 0. \quad (A9)$$

From Eqn. (A7),

$$\left(\frac{\partial}{\partial t} + \frac{1}{\tau_0} \right) \mathbf{j}(\mathbf{r}, t) = \frac{\epsilon_\infty \omega_p^2}{4\pi} \mathbf{E}(\mathbf{r}, t) - \frac{\epsilon_\infty}{4\pi} e^{-\frac{t}{\tau_0}} \times \left[\mathbf{M}(t, t) \mathbf{E}(\mathbf{r}, t) + \int_{-\infty}^t dt' \frac{\partial \mathbf{M}(t, t')}{\partial t} \cdot \mathbf{E}(\mathbf{r}, t') \right] \quad (\text{A10})$$

so that we can express (A9) as the Wave Equation

$$\begin{aligned} & \left(\frac{\partial}{\partial t} + \frac{1}{\tau_0} \right) \left(\frac{\partial^2 \mathbf{E}}{\partial t^2} + \frac{c^2}{\epsilon_\infty} \operatorname{curl} \operatorname{curl} \mathbf{E} \right) + \omega_p^2 \frac{\partial \mathbf{E}}{\partial t} \\ &= \frac{\partial}{\partial t} \left[\mathbf{M}_0 \cdot \mathbf{E} + e^{-\frac{t}{\tau_0}} \int_{-\infty}^t dt' \frac{\partial \mathbf{M}}{\partial t} \cdot \mathbf{E}(t') \right], \quad (\text{A11}) \end{aligned}$$

where

$$\mathbf{M}_0(t) \equiv \mathbf{M}(t, t) e^{-\frac{t}{\tau_0}}. \quad (\text{A12})$$

Appendix B: Boundary Conditions at a Time Interface

The original wave equation (A9) that is a direct consequence of the full set of Maxwell's Equations, implies the continuity of the electric field $\mathbf{E}(t)$ and the field

$$\mathbf{G} \equiv \frac{\partial \mathbf{E}}{\partial t} - \frac{4\pi}{\epsilon_\infty} \mathbf{j}. \quad (\text{B1})$$

Substituting (A7) into (B1), we find

$$\mathbf{G} = \mathbf{F} + \omega_p^2 \int_{-\infty}^t dt' e^{-\frac{t-t'}{\tau_0}} \mathbf{E}(t'), \quad (\text{B2})$$

where the auxiliary field

$$\mathbf{F} \equiv \frac{\partial \mathbf{E}}{\partial t} - e^{-\frac{t}{\tau_0}} \int_{-\infty}^t dt' \mathbf{M}(t, t') \cdot \mathbf{E}(\mathbf{r}, t'). \quad (\text{B3})$$

Therefore, together with the already established continuity of the electric field \mathbf{E} , Eqn. (B3) implies the continuity of the auxiliary "time displacement field" \mathbf{F} .

Then the wave equation (22) can be expressed as

$$\begin{aligned} & \frac{\partial}{\partial t} \left[\frac{\partial \mathbf{F}}{\partial t} + \frac{\mathbf{F}}{\tau_0} \right] + \frac{\partial}{\partial t} \left[\frac{c^2}{\epsilon_\infty} \operatorname{curl} \operatorname{curl} \mathbf{E} + \omega_p^2 \mathbf{E} \right] \\ &+ \frac{1}{\tau_0} \operatorname{curl} \operatorname{curl} \mathbf{E} = 0, \quad (\text{B4}) \end{aligned}$$

which implies the continuity of the derivative $\partial \mathbf{F} / \partial t$.

Therefore, the complete set of three boundary conditions at a time interface, corresponds to the continuity of the electric field \mathbf{E} , the time displacement field \mathbf{F} and the first (time) derivative of the time displacement field $\partial \mathbf{F} / \partial t$.

Appendix C: Wave Equation in the Lossless Limit

In the nearly-lossless limit $\omega \tau_0 \gg 1$, we can neglect the scattering term in the kinetic equations (4) and (18), which yields

$$f_M(\mathbf{p}, t) = f_0(\mathbf{p} - \mathbf{p}_D(t)), \quad (\text{C1})$$

and

$$g = \frac{\partial f_0(\mathbf{p} - \mathbf{p}_M(t))}{\partial \mathbf{p}} \int_{-\infty}^t dt' e \mathbf{E}(t), \quad (\text{C2})$$

so that the current density due to the signal field \mathbf{E} is given by

$$\mathbf{j}(\mathbf{r}, t) = \frac{\epsilon_\infty \omega_p^2}{4\pi} \frac{m_*}{\mathbf{m}_M} \int_{-\infty}^t dt' e \mathbf{E}(\mathbf{r}, t'), \quad (\text{C3})$$

with the time-dependent effective mass defined as

$$\left[\frac{m_*}{\mathbf{m}_M(t)} \right]_{\alpha\beta} = \frac{\langle \frac{\partial^2 \varepsilon_{\mathbf{p}+\mathbf{p}_M(t)}}{\partial p_\alpha \partial p_\beta} \rangle_{\mathbf{p}}}{\langle \frac{\partial^2 \varepsilon_{\mathbf{p}}}{\partial p^2} \rangle_{\mathbf{p}}}. \quad (\text{C4})$$

Substituting (C3) into (A9), we obtain the wave equation (33).

Appendix D: Electronic Band Non-parabolicity

An accurate description for a non-parabolic band [26] in an optoelectronic material can be obtained from the celebrated Kane model [30] that originates from a perturbation approach to the solution of the Schrödinger equation of a single electron in a crystal potential including the spin-orbit interaction:

$$\varepsilon_{\mathbf{p}}(1 + \alpha_* \varepsilon_{\mathbf{p}}) = \frac{p^2}{2m_0}, \quad (\text{D1})$$

where the (temperature-dependent) parameter α is on the order of (and in some cases such e.g., bismuth and its alloys, equal to) the inverse bandgap energy $\alpha_* \sim E_g^{-1}$. While highly accurate for the direct bandgap III-V semiconductors of cubic symmetry and their alloys, the Kane model (D1) can also be used at the quantitative level for many other materials [39–42].

With the Kane's expression for $\varepsilon_{\mathbf{p}}$, we obtain

$$\frac{\partial^2 \varepsilon}{\partial p_\alpha \partial p_\beta} = \frac{1}{m_0} \left[\frac{\delta_{\alpha\beta}}{1 + 2\alpha_* \varepsilon_{\mathbf{p}}} - \frac{2\alpha_* p_\alpha p_\beta}{m_0 (1 + 2\alpha_* \varepsilon_{\mathbf{p}})^3} \right]. \quad (\text{D2})$$

so that for the induced anisotropy in the dielectric permittivity (41) we find

$$\frac{\Omega_\parallel^2 - \Omega_\perp^2}{\omega_p^2} = 2 \frac{\alpha_*}{m_0} \sum_{t_n < t} e^{-\frac{t-t_n}{\tau_0}} \Delta p_n^2 (1 - \Delta_n), \quad (\text{D3})$$

where

$$\begin{aligned}\Delta_n &= \frac{e^2}{2\pi^2\hbar^3\epsilon_\infty\omega_p^2} \int d\mathbf{p} \frac{f_0(\mathbf{p} - \Delta\mathbf{p}_n) - f_0(\mathbf{p})}{\Delta p_n^2} \\ &\times \left(p^2 - \frac{3(\mathbf{p} \cdot \Delta\mathbf{p}_n)^2}{\Delta p_n^2} \right) \left(1 - \frac{1}{(1 + 2\alpha_*\varepsilon_p)^3} \right) \quad (\text{D4})\end{aligned}$$

$$= \mathcal{O}(\alpha_*\varepsilon_F) = \mathcal{O}\left(\frac{\varepsilon_F}{E_g}\right), \quad (\text{D5})$$

and the subscripts correspond to the directions parallel (||) and perpendicular (⊥) to the *pump* field \mathbf{E}_M modulating the material.

In the limit of moderate carrier drift modulation, $\Delta p_n < p_F$, we find

$$\Omega_{\parallel}^2 \simeq 3\frac{\alpha_*\omega_p^2}{m_0} \sum_{t_n < t} \Delta p_n^2 e^{-\frac{t-t_n}{\tau_0}}, \quad (\text{D6})$$

$$\Omega_{\perp}^2 \simeq \frac{\alpha_*\omega_p^2}{m_0} \sum_{t_n < t} \Delta p_n^2 e^{-\frac{t-t_n}{\tau_0}}. \quad (\text{D7})$$

Appendix E: Time-Reflection and Time-Transmission Coefficients – general treatment

Close to the time interface at $t = 0$ (i.e. for $t \ll \tau_0$) with a single monochromatic incident wave (47), the auxiliary field \mathbf{F} and its derivative are given by

$$\begin{aligned}\mathbf{F} &= \frac{\partial \mathbf{E}}{\partial t} - \Omega_{\perp}^2 \theta(t) \int_{-\infty}^0 dt' e^{t'/\tau_0} \mathbf{E}(t') \\ &= \frac{\partial \mathbf{E}}{\partial t} - \frac{\Omega_{\perp}^2 \tau_0}{1 - i\omega\tau_0} \theta(t) \mathbf{E}, \quad (\text{E1})\end{aligned}$$

$$\begin{aligned}\frac{\partial \mathbf{F}}{\partial t} &= \frac{\partial^2 \mathbf{E}}{\partial t^2} - \Omega_{\perp}^2 \theta(t) \left(\mathbf{E} - \int_{-\infty}^0 \frac{dt'}{\tau_0} e^{t'/\tau_0} \mathbf{E}(t') \right) \\ &= \frac{\partial^2 \mathbf{E}}{\partial t^2} - \frac{\Omega_{\perp}^2}{1 + \frac{i}{\omega\tau_0}} \theta(t) \mathbf{E}. \quad (\text{E2})\end{aligned}$$

Using the continuity of the fields \mathbf{E} , \mathbf{F} and $\partial\mathbf{F}/\partial t$ (see Eqn. (30) in Section III) at the temporal interface $t = 0$, from Eqns. (47), (E1), (E2) and (62) we obtain

$$\mathcal{T} + \mathcal{R} + \mathcal{S} = 1, \quad (\text{E3})$$

$$\begin{aligned}\left(\omega' - \frac{i\gamma}{\tau_0}\right) \mathcal{T} + \left(-\omega' - \frac{i\gamma}{\tau_0}\right) \mathcal{R} - i\frac{1-2\gamma}{\tau_0} \mathcal{S} \\ = \omega \left(1 - \frac{\Omega_{\perp}^2}{\omega(\omega + i/\tau_0)}\right), \quad (\text{E4})\end{aligned}$$

$$\begin{aligned}\left(\omega' - \frac{i\gamma}{\tau_0}\right)^2 \mathcal{T} + \left(\omega' + \frac{i\gamma}{\tau_0}\right)^2 \mathcal{R} - \frac{(1-2\gamma)^2}{\tau_0^2} \mathcal{S} \\ = \omega^2 \left(1 - \frac{\Omega_{\perp}^2}{\omega(\omega + i/\tau_0)}\right) \quad (\text{E5})\end{aligned}$$

or equivalently

$$\begin{aligned}\mathcal{W}_3 \left[\omega' - \frac{i\gamma}{\tau_0}, -\omega' - \frac{i\gamma}{\tau_0}, -i\frac{(1-2\gamma)}{\tau_0} \right] \begin{pmatrix} \mathcal{T} \\ \mathcal{R} \\ \mathcal{S} \end{pmatrix} \\ = \begin{pmatrix} 1 \\ \eta_\omega \omega \\ \eta_\omega \omega^2 \end{pmatrix}, \quad (\text{E6})\end{aligned}$$

where

$$\eta_\omega \equiv 1 - \frac{\Omega_{\perp}^2}{\omega(\omega + i/\tau_0)}, \quad (\text{E7})$$

and \mathcal{W}_3 is the 3rd order Vandermonde matrix [43]

$$\mathcal{W}_3(x_0, x_1, x_2) \equiv \begin{bmatrix} 1 & 1 & 1 \\ x_0 & x_1 & x_2 \\ x_0^2 & x_1^2 & x_2^2 \end{bmatrix} \quad (\text{E8})$$

with the determinant

$$\det \mathcal{W}_3 = (x_0 - x_1)(x_0 - x_2)(x_1 - x_2), \quad (\text{E9})$$

and the inverse

$$\begin{aligned}\mathcal{W}_3^{-1} &= \frac{1}{\det \mathcal{W}_3} \\ &\times \begin{bmatrix} x_1 x_2 (x_2 - x_1) & x_1^2 - x_2^2 & x_2 - x_1 \\ x_0 x_2 (x_0 - x_2) & x_0^2 - x_2^2 & x_0 - x_2 \\ x_0 x_1 (x_1 - x_0) & x_0^2 - x_1^2 & x_1 - x_0 \end{bmatrix} \quad (\text{E10})\end{aligned}$$

We therefore obtain

$$\mathcal{R} = \frac{\eta_\omega \omega (\omega - \omega' + i\frac{1-\gamma}{\tau_0}) - i\frac{1-2\gamma}{\tau_0} (\omega' - i\frac{\gamma}{\tau_0})}{2\omega' (\omega' - i\frac{1-3\gamma}{\tau_0})}, \quad (\text{E11})$$

$$\mathcal{T} = \frac{\eta_\omega \omega (\omega + \omega' + i\frac{1-\gamma}{\tau_0}) + i\frac{1-2\gamma}{\tau_0} (\omega' + i\frac{\gamma}{\tau_0})}{2\omega' (\omega' + i\frac{1-3\gamma}{\tau_0})}, \quad (\text{E12})$$

$$\mathcal{S} = \frac{\omega'^2 - \eta_\omega \omega (\omega + 2i\gamma/\tau_0) + \gamma^2/\tau_0^2}{\omega'^2 + (1-3\gamma)^2/\tau_0^2}, \quad (\text{E13})$$

Appendix F: Time-Reflection and Time-Transmission Coefficients – lossless limit

In the lossless limit $\omega\tau_0 \gg 1$ the wave equation (33) is of the second order in time, so that the time-evanescent field is decoupled from the propagating waves and is not excited at a temporal interface. When the modulation pulse applied at $t = 0$, for the electric field we therefore obtain

$$\mathbf{E}(\mathbf{r}, t) = \mathbf{E}_0 e^{i\mathbf{k} \cdot \mathbf{r}} \begin{cases} e^{-i\omega t}, & t < 0 \\ \mathcal{T} e^{-i\omega' t} + \mathcal{R} e^{i\omega' t}, & t > 0. \end{cases} \quad (\text{F1})$$

where (see also Eqns. (15), (16))

$$\omega = \sqrt{\omega_p^2 + \frac{k^2 c^2}{\epsilon_\infty}}, \quad (\text{F2})$$

$$\omega' = \sqrt{\frac{m_*}{m_M} \omega_p^2 + \frac{k^2 c^2}{\epsilon_\infty}}. \quad (\text{F3})$$

and, in the coordinates of Fig. 1,

$$m_M = [\mathbf{m}_M(t > 0)]_{zz} \equiv \left\langle \frac{\partial^2 \varepsilon_{\mathbf{p}+\mathbf{p}_M}}{\partial p_z^2} \right\rangle_{\mathbf{p}}^{-1}. \quad (\text{F4})$$

Then

$$\int_{-\infty}^0 dt' \mathbf{E}(t') = - \frac{\mathbf{E}_0 e^{i\mathbf{k}\cdot\mathbf{r}}}{i\omega}, \quad (\text{F5})$$

and the temporal displacement at the time interface $t = 0$

$$\mathbf{F} = \mathbf{E}_0 e^{i\mathbf{k}\cdot\mathbf{r}} \begin{cases} -i\omega \left[1 - \frac{\omega_p^2}{\omega^2} \right], & t = -0, \\ -i\omega' \left[\mathcal{T} - \mathcal{R} - \frac{m_*}{m_M} \frac{\omega_p^2}{\omega'^2} \right], & t = +0. \end{cases} \quad (\text{F6})$$

Using the continuity of the electric field \mathbf{E} and the time displacement \mathbf{F} at $t = 0$, we obtain

$$\mathcal{T} = \frac{1}{2} + \frac{\omega^2 - \omega_p^2 \left(1 - \frac{m_*}{m_M} \right)}{2\omega\omega'}, \quad (\text{F7})$$

$$\mathcal{R} = \frac{1}{2} - \frac{\omega^2 - \omega_p^2 \left(1 - \frac{m_*}{m_M} \right)}{2\omega\omega'}. \quad (\text{F8})$$

From Eqns. (F2),(F3)

$$\omega'^2 = \omega^2 - \omega_p^2 \left(1 - \frac{m_*}{m_M} \right), \quad (\text{F9})$$

which reduces Eqns. (F7),(F8) to

$$\mathcal{T} = \frac{\omega + \omega'}{2\omega}, \quad (\text{F10})$$

$$\mathcal{R} = \frac{\omega - \omega'}{2\omega}. \quad (\text{F11})$$

Appendix G: Wave Equation in the Quasistatic Limit

From the Gauss Law

$$\epsilon_{\infty} \operatorname{div} \mathbf{E} = 4\pi\rho \quad (\text{G1})$$

and the conservation of free charge

$$\frac{\partial \rho}{\partial t} + \operatorname{div} \mathbf{j} = 0, \quad (\text{G2})$$

we obtain

$$\epsilon_{\infty} \frac{\partial}{\partial t} \nabla^2 \phi = 4\pi \nabla \cdot \mathbf{j}. \quad (\text{G3})$$

Introducing the Fourier representation of the scalar potential

$$\phi(\mathbf{r}, t) = \int \phi_{\mathbf{k}}(t) e^{i\mathbf{k}\cdot\mathbf{r}}, \quad (\text{G4})$$

and substituting Eqn. (A7) into (G3), we obtain

$$\begin{aligned} e^{\frac{t}{\tau_0}} \frac{d\phi_{\mathbf{k}}}{dt} + \omega_p^2 \int_{-\infty}^t dt' \phi_{\mathbf{k}}(t') e^{\frac{t'}{\tau_0}} \\ = \int_{-\infty}^t dt' \mathcal{M}_{\mathbf{k}}(t, t') \phi_{\mathbf{k}}(t'), \end{aligned} \quad (\text{G5})$$

where the (scalar) modulation kernel $\mathcal{M}_{\mathbf{k}}(t)$ is given by

$$\mathcal{M}_{\mathbf{k}}(t, t') = \frac{\mathbf{k} \cdot \mathbf{M}(t, t') \cdot \mathbf{k}}{k^2}. \quad (\text{G6})$$

For the wave equation in the quasistatic limit we therefore obtain

$$\begin{aligned} \frac{d^2 \phi_{\mathbf{k}}}{dt^2} + \frac{1}{\tau_0} \frac{d\phi_{\mathbf{k}}}{dt} + \left(\omega_p^2 - \mathcal{M}_{\mathbf{k}}^{(0)}(t) \right) \phi_{\mathbf{k}} \\ = e^{-\frac{t}{\tau_0}} \int_{-\infty}^t dt' \frac{\partial \mathcal{M}_{\mathbf{k}}}{\partial t} \phi_{\mathbf{k}}(t'), \end{aligned} \quad (\text{G7})$$

where

$$\mathcal{M}_{\mathbf{k}}^{(0)}(t) \equiv e^{-\frac{t}{\tau_0}} \mathcal{M}_{\mathbf{k}}(t, t). \quad (\text{G8})$$

[1] E. Goulielmakis, M. Schultze, M. Hofstetter, V. S. Yakovlev, J. Gagnon, M. Uiberacker, A. L. Aquila, E. M. Gullikson, D. T. Attwood, R. Kienberger, F. Krausz, and U. Kleineberg, Single-Cycle Nonlinear Optics, *Science* **320** (5883), 1614 - 1617 (2008).

[2] R. Morgenthaler, Velocity modulation of electromagnetic waves. *IRE Trans. Microw. Theory Tech.* **6**, 167 - 172 (1958).

[3] J. T. Mendonça and P. K. Shukla, Time Refraction and Time Reflection: Two Basic Concepts, *Phys. Scr.* **65**, 160 (2002).

[4] F. Biancalana, A. Amann, A. V. Uskov, and E. P. O'Reilly, Dynamics of light propagation in spatiotemporal dielectric structures, *Phys. Rev. E* **75** (4), 046607 (2007).

[5] J. R. Zurita-Sánchez, P. Halevi, and J. C. Cervantes-González, Reflection and transmission of a wave incident on a slab with a time-periodic dielectric function $\epsilon(t)$, *Phys. Rev. A* **79** (5), 053821 (2009).

[6] J. R. Zurita-Sánchez, J. H. Abundis-Patiño, and P. Halevi, Pulse propagation through a slab with time-periodic dielectric function $\epsilon(t)$, *Opt. Express* **20**, 5586 -

5600 (2012).

[7] A. M. Shaltout, J. Fang, A. V Kildishev, and V. M. Shalaev, Photonic Time-Crystals and Momentum Band-Gaps, in Conference on Lasers and Electro-Optics (Optica Publishing Group), FM1D.4 (2016).

[8] E. Lustig, Y. Sharabi, and M. Segev, Topological aspects of photonic time crystals, *Optica* **5**(11), 1390 - 1395 (2018).

[9] E. Lustig, O. Segal, S. Saha, C. Fruhling, V. M. Shalaev, A. Boltasseva, and M. Segev, Photonic time-crystals - fundamental concepts,' *Opt. Express* **31**, 9165 - 9170 (2023).

[10] S. Saha, O. Segal, C. Fruhling, E. Lustig, M. Segev, A. Boltasseva, and V. M. Shalaev, Photonic time crystals: a materials perspective, *Opt. Express* **31**, 8267 - 8273 (2023).

[11] H. Li, S. Yin, H. He, J. Xu, A. Alù, and B. Shapiro, Stationary Charge Radiation in Anisotropic Photonic Time Crystals, *Phys. Rev. Lett.* **130**, 093803 (2023).

[12] J. Feinberg, D. E. Fernandes, B. Shapiro, and M. G. Silveirinha, Plasmonic Time Crystals, *Phys. Rev. Lett.* **134**, 183801 (2025).

[13] Khurgin, J. B. Energy and Power Requirements for Alteration of the Refractive Index. *Laser & Photonics Reviews* **18** (4), 2300836 (2024).

[14] N. I. Zheludev, Polarization instability and multistability in nonlinear optics. *Sov. Phys. Usp.* **32**, 357 (1989).

[15] H. N. S. Krishnamoorthy *et al.*, Topological Transitions in Metamaterials. *Science* **336**, 205 - 209 (2012).

[16] V. A. Podolskiy and E. E. Narimanov, Strongly anisotropic waveguide as a nonmagnetic left-handed system. *Phys. Rev. B* **71**, 201101(R) (2005).

[17] S. D. Gorelov, A. L. Novokovskaya, S. B. Bodrov, M. V. Sarafanova, M. I. Bakunov, Unipolar fields produced by ultrafast optical gating of terahertz pulses. *Applied Physics Letters* **126**(1), 011104 (2025).

[18] J. M. Ziman, *Electrons and Phonons: The Theory of Transport Phenomena in Solids*, (Oxford University Press, Reprint edition, 2001).

[19] L. I. Pitaevskii and E. M. Lifshitz *Physical Kinetics*, (Butterworth-Heinemann, 1st ed.; 1981).

[20] E. Lustig, O. Segal, S. Saha, E. Bordo, S. N. Chowdhury, Y. Sharabi , A. Fleischer , A. Boltasseva, O. Cohen , V. M. Shalaev and M. Segev, Time-refraction optics with single cycle modulation,' *Nanophotonics* **12** (12), 2221 - 2230 (2023).

[21] Jaffray, W.; Saha, S.; Shalaev, V. M.; Boltasseva, A. and Ferrera, M. Transparent conducting oxides: from all-dielectric plasmonics to a new paradigm in integrated photonics,. *Advances in Optics and Photonics* **14** (2), 148 - 208 **2022**.

[22] Kim, T. S.; Choi, C. H.; Jeong, T. S. and Shim, K. H. Influence of Substrate Temperature and O₂ Flow on the Properties of RF-Magnetron-Sputtered Indium-Tin-Oxide Thin Films. *J. Korean Phys. Soc.*,**51** (2), 534 - 538 (2007).

[23] Hoffman, A. J.; Alekseyev, L.; Howard, S. S.; Franz, K. J.; Wasserman, D. M.; Podolskiy, V. A.; Narimanov, E. E.; Sivco, D. L.; Gmachl, C. Negative refraction in semiconductor metamaterials. *Nature Materials* **6**, 946 - 950 (2007).

[24] J. E. Medvedeva, Magnetically Mediated Transparent Conductors: In₂O₃ doped with Molybdenum. *Phys. Rev. Lett.* **97**, 086401 (2006).

[25] X. Liu, J.-H. Park, J.-H. Kang, H. Yuan, Y. Cui, H. Y. Hwang, and M. L. Brongersma, Quantification and Impact of nonparabolicity of the conduction band of indium tin oxide on its plasmonic properties, *Appl. Phys. Lett.* **105**, 181117 (2014).

[26] M. Balkaitiski and E. Amzallag, Band Parameters Determination from Faraday Rotation Measurements. *Phys. Stat. Sol.* **30**, 407 (1968).

[27] M. Cardona, *Phys. Rev.* **121**, 752 (1961).

[28] H. Piller, (Kyoto Conf. Semiconductors), *J. Phys. Soc. Japan* **21**, Suppl., 206 (1966).

[29] S. G. Shulman and Yu. I. Ukhanov, *Soviet Phys. - Solid State* **7**, 768 (1965).

[30] E. O. Kane, Band structure of indium antimonide. *J. Phys. Chem. Solids* **1**, 249 - 261 (1957).

[31] S. Ramo, J. R. Whinnery, T. Van Duzer, *Fields and Waves in Communication Electronics*, (Wiley, 3rd edition, 1994).

[32] E.g., for heavily doped semiconductors used in near to mid infrared (IR) range such as GaAs [23] , $c\tau_0 \sim 100 \mu\text{m}$, while in transparent conducting oxides (wavelengths in visible to near IR) such as ITO [24], $c\tau_0 \sim 10 \mu\text{m}$. In both cases the length $c\tau_0$ exceeds the corresponding values of $1/k \sim \lambda_0$, (where λ_0 is the free-space signal wavelength) by more than an order of magnitude.

[33] E. E. Narimanov, Photonic Hypercrystals. *Physical Review X* **4**, 041014 (2014).

[34] J.W. Strutt (Lord Rayleigh), On the maintenance of vibrations by forces of double frequency, and on the propagation of waves through a medium endowed with periodic structure. *Philosophical Magazine* (5th series) **24** (147), 145 - 159 (1887).

[35] T.G. Roer, *Microwave Electronic Devices*, (Springer Science and Business Media, 2012).

[36] L. D. Landau and E. M. Lifshitz, *Electrodynamics of Continuous Media*, (Pergamon Press, 2nd edition, 1984).

[37] F. Capasso, K. Mohammed, A. Y. Cho, R. Hull, A. L. Hutchinson, Effective mass filtering: Giant quantum amplification of the photocurrent in a semiconductor superlattice. *Appl. Phys. Lett.* **47**, 420-422 (1985).

[38] N. Lenke, P. Steinleitner, M. Kowalczyk, Philipp Rosenberger, S. Gröbmeyer, A. Sebesta, V. Pervak, N. Karpowicz, F. Krausz, and A. Weigel, Single-cycle CEP-stable Cr:ZnS lasers. *EPJ Web of Conferences* **307**, 04036 (2024).

[39] W. Zawadzki, Electron transport phenomena in small-gap semiconductors. *Adv. Phys.* **23**, 435 - 522 (1973).

[40] N. W. Ashcroft and N. D. Mermin, *Solid State Physics* (Philadelphia: Saunders College,1976).

[41] M. A. Green, Intrinsic concentration, effective densities of states, and effective mass in silicon. *J. Appl. Phys.* **67**, 2944 - 2954 (1990).

[42] R. A. Masut, Highlighting non-parabolic bands in semiconductors. *Eur. J. Phys.* **43**, 015501 (2022).

[43] N. Macon, A. Spitzbart, Inverses of Vandermonde Matrices". *The American Mathematical Monthly* **65** (2), 95 - 100 (1958).